

Photochemical C(sp)–C(sp²) Bond Activation in Phosphaalkynes: A New Route to Reactive Terminal Cyaphido Complexes L_nM–C≡P

Tim Görlich, Daniel S. Frost, Nico Boback, Nathan T. Coles, Birger Dittrich, Peter Müller, William D. Jones,* and Christian Müller*

Cite This: *J. Am. Chem. Soc.* 2021, 143, 19365–19373

Read Online

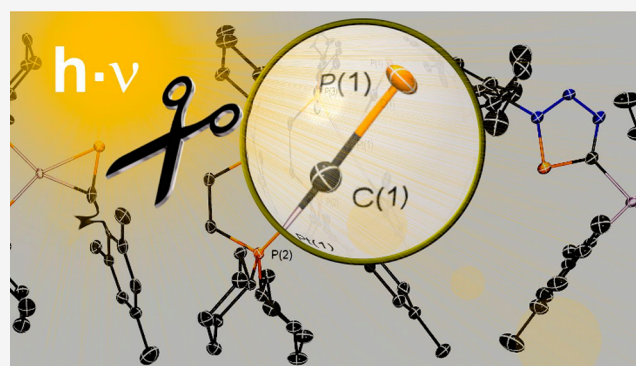
ACCESS |

Metrics & More

Article Recommendations

Supporting Information

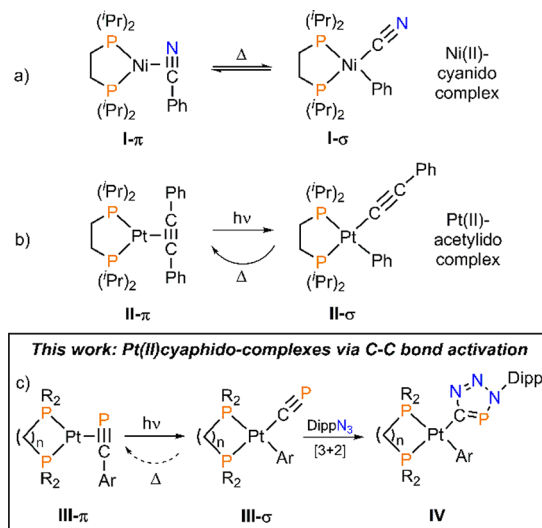
ABSTRACT: The photochemical activation of the C(sp)–C(sp²) bond in Pt(0)-η²-aryl-phosphaalkyne complexes leads selectively to coordination compounds of the type L_nPt(aryl)(C≡P). The oxidative addition reaction is a novel, clean, and atom-economic route for the synthesis of reactive terminal Pt(II)-cyaphido complexes, which can undergo [3 + 2] cycloaddition reactions with organic azides, yielding the corresponding Pt(II)-triazaphospholato complexes. The C–C bond cleavage reaction is thermodynamically uphill. Upon heating, the reverse and quantitative reductive elimination toward the Pt(0)-phosphaalkyne-π-complex is observed.



1. INTRODUCTION

Cyanido complexes represent an important class of coordination compounds in various domains of chemistry, ranging from fundamental aspects of bonding to applications in material science.¹ As an excellent σ-donor and strong π-acceptor ligand, the cyanide anion CN[−] can adopt both a terminal M–CN as well as a bridging M–CN–M' coordination mode. This leads to a plethora of mono- and polycyanido complexes with interesting coordination geometries and physicochemical properties. Cyanido complexes are typically prepared by salt metathesis reactions, using a suitable chlorido complex and MCN (M = alkali metal). Moreover, the oxidative addition of HCN to L_nNi(0), forming L_nNi(H)CN complexes, is a crucial step in the industrially relevant Ni-catalyzed hydrocyanation of alkenes.² Also, metal mediated activation of C–C bonds in nitriles (R–CN) leads to cyanido complexes.³ In 2000, Garcia and Jones investigated the reversible thermal cleavage of the C(sp)–C(sp²) bond in benzonitrile with Ni(0) (Chart 1a).⁴ This observation is particularly impressive, considering benzonitrile has a C–CN bond dissociation energy of 132.7 kcal/mol. Soon after, this concept was transferred to the C(sp)–C(sp²) bond cleavage in diphenylacetylene with Pt(0) (Chart 1b).⁵ Upon photolysis of the diphenylacetylene Pt(0)-π-complex II-π, the oxidative addition reaction proceeds quantitatively within several hours to the Pt(II)-complex II-σ. By means of quantum chemical calculations, Weigand, González and co-workers investigated the first step of the mechanism of this photochemical bond activation process for a series of Pt(0)-diphenylacetylene complexes.⁶ Interestingly, the rather slow back reaction II-σ → II-π proceeds thermally at

Chart 1. C(sp)–C(sp²) Bond Activation Reactions and Brief Summary of This Work



Received: July 15, 2021

Published: November 10, 2021



temperatures around $T = 125\text{ }^{\circ}\text{C}$.^{6,7} This reverse reaction indicates that the photochemical oxidative addition of the $\text{C}(sp)\text{-C}(sp^2)$ bond is thermodynamically uphill. It should also be mentioned that analogous $\text{Ni}(0)$ -diphenylacetylene complexes do not show any C-C bond activation reactions, neither photochemically nor thermally.

From a conceptual point of view, phosphalkynes are valence isoelectronic to nitriles. Moreover, the diagonal relationship in the periodic table of the elements between phosphorus and carbon is particularly reflected in pronounced similarities between unsaturated hydrocarbons and low-coordinate organophosphorus compounds.⁸ Thus, the analogous and hitherto unknown $\text{C}(sp)\text{-C}(sp^2)$ bond activation in aryl-substituted phosphalkynes could lead to cyaphido complexes of the type $\text{L}_n\text{M-C}\equiv\text{P}$ (**III- σ** , Chart 1c).

In fact, cyaphido complexes are rather rare, as only a limited number of synthetic protocols are available and, additionally, because $\text{MC}\equiv\text{P}$ salts ($\text{M} = \text{alkali metal}$) are unknown. Consequently, the cyaphido ligand has to be generated in the coordination sphere of a metal complex. The first $\text{Pt(II)-C}\equiv\text{P}$ complex was presented in 1992 by Angelici et al. but could only be characterized spectroscopically due to its instability.⁹ The first coordination compound with a terminal $\text{C}\equiv\text{P}^-$ ligand which could be characterized crystallographically was reported by Grützmacher and co-workers in 2006.¹⁰ The $\text{Ru(II)-C}\equiv\text{P}$ complex was obtained *via* base-induced desilylating rearrangement of an $\eta^1\text{-Ph}_3\text{Si-C}\equiv\text{P-Ru(II)}$ complex. To date, this synthetic strategy is still the most common route to generate $\text{Ru(II)-C}\equiv\text{P}$ complexes. In an adapted version of this protocol, Crossley and co-workers used $\text{Me}_3\text{Si-C}\equiv\text{P}$ to generate analogous $\text{Ru(II)-C}\equiv\text{P}$ complexes.¹¹ A similar synthetic principle was described by Russell et al. in 2012. Instead of PhO^- or tBuO^- , $[\text{NBu}_4][\text{Ph}_3\text{SiF}_2]$ was used for the desilylation reaction, resulting in the formation of the terminal $\text{C}\equiv\text{P}^-$ ligand.¹² The cyaphido-based Lewis pair $[(\text{CF}_3)_3\text{B} \leftarrow \text{C}\equiv\text{P}][\text{PPh}_4]$ was described in 2004 by Willner and co-workers.¹³ This compound is isoelectronic (B^-/C) to the corresponding neutral phosphalkyne, and its synthesis proceeds analogously as described by Becker et al.¹⁴ The first example of coordination compounds consisting of an actinide metal and a terminal $\text{C}\equiv\text{P}^-$ ligand is a $\text{U(IV)-C}\equiv\text{P}$ complex recently reported by Meyer and co-workers.¹⁵ The formation of the cyaphido ligand proceeds by reductive C-O bond cleavage of a σ -coordinating phosphoethynolate (OCP^-) anion by a strongly oxophilic U(III) center. Based on this approach, Goichoechea and co-worker recently developed the $\text{C}\equiv\text{P}^-$ -transfer reagent $[\text{Mg}(\text{DippNacNac})(\text{CP})(\text{dioxane})]$, starting from $\text{tPr}_3\text{SiOC}\equiv\text{P}$ and a magnesium(I) reagent.¹⁶ In this way, Ge- , Sn- , and Au(I)-cyaphido complexes could be synthesized for the first time. However, all these cyaphido complexes suffer from a rather high thermal and kinetic stability and no follow-up reactions at the $\text{C}\equiv\text{P}$ moiety occur.

Taking the limited access to $\text{L}_n\text{M-C}\equiv\text{P}$ complexes into account, we anticipated that the $\text{C}(sp)\text{-C}(sp^2)$ bond activation reaction in π -bound aryl-phosphalkynes (**III- π**) might thus be an elegant new procedure to access novel cyaphido complexes of the type **III- σ** (Chart 1c). In fact, the two quasi-degenerate HOMOs of a phosphalkyne are π -orbitals, the respective free electron pair is energetically lower (HOMO-2), and the $n\text{-}\pi$ -separation is relatively large. This orbital arrangement leads to preferential η^2 -coordination of the $\text{C}\equiv\text{P}$ triple bond, particularly to electron-rich metal centers, which would be a prerequisite for our approach.¹⁷

2. RESULTS AND DISCUSSION

As $\text{Ph-C}\equiv\text{P}$ is rather unstable and the synthesis is not trivial, we focused on the aryl-phosphalkynes **1-3** (Figure 1).

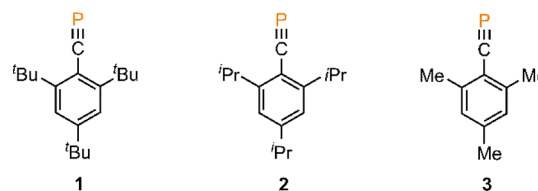


Figure 1. Aryl-substituted phosphalkynes used in this study.

However, the steric demand of $\text{Mes}^*\text{-C}\equiv\text{P}$ (**1**) also had to be taken into account, which could prevent formation of π -complexes and the subsequent C-C bond activation reaction. Nevertheless, **1** is easy to synthesize and is relatively kinetically, as well as thermodynamically, stable.¹⁸ Compound **1** would thus be an ideal starting material for our investigations. $\text{Mes-C}\equiv\text{P}$ (**3**), on the other hand, is both less thermodynamically and kinetically stable than **1** and should be more similar to $\text{Ph-C}\equiv\text{P}$. This was demonstrated by Scheer and co-workers, who reported the coordination compound $((\text{PPh}_3)_2\text{Pt-}\eta^2(\text{Mes-C}\equiv\text{P}))$ in 2004.¹⁹

In terms of stability and steric demand, phosphalkyne **2** is expected to be in between **1** and **3**. Phosphalkynes **1** and **3**, as well as the 1,3,5-triisopropylphenyl-substituted phosphalkyne Tripp-C≡P (**2**), were synthesized on multigram scale according to modified literature procedures.¹⁹ At ambient conditions, compound **3** is a colorless oil with a freezing point of $T = 10.5\text{ }^{\circ}\text{C}$. We were able to grow crystals of **3**, and the result of the X-ray crystal structure analysis is shown in Figure 2, along with selected bond lengths and angles.

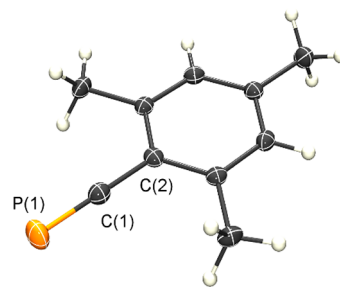
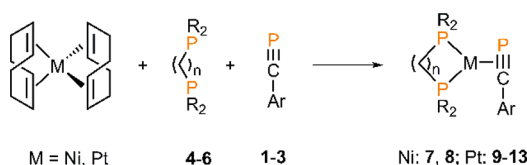


Figure 2. Molecular structure of **3** in the crystal. The asymmetric unit consists of two halves of **3**, only one is shown. Displacement ellipsoids are shown at the 50% probability level. The following symmetry operation was used to generate the crystallographically related atoms: $2 - x, 1 - x + y, 4/3 - z$. Selected bond lengths (Å) and angles (deg): $\text{P(1)-C(1)}, 1.545(3)$; $\text{P(2)-C(8)}, 1.547(3)$; $\text{C(1)-C(2)}, 1.432(4)$; $\text{C(8)-C(9)}, 1.431(4)$. $\text{P(1)-C(1)-C(2)}, 180.00$; $\text{P(2)-C(8)-C(9)}, 180.00$.

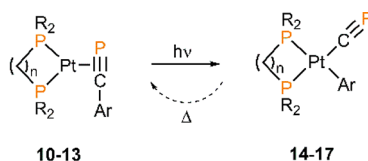
As coligands for the envisaged $\text{Ni}(0)$ - and $\text{Pt}(0)$ -phosphalkyne- π -complexes, we chose chelating diphosphines **4-6**, which have differing steric demand in the R-substituents (*i*Pr, Cy) as well as bite angles ($n = 1, 2$, Scheme 1). Moreover, **4-6** are much stronger σ -donors than aryl-substituted phosphines, which would help promote the oxidative addition to the metal centers. Upon reacting $\text{Ni}(\text{cod})_2$ or $\text{Pt}(\text{cod})_2$ with the diphosphine and the phosphalkyne in a ratio of 1:1:1, we were able to access the η^2 -phosphalkyne complexes **7-13** (Scheme 2). All coordination compounds could be isolated as

Scheme 1. Synthesis of Ni(0)- and Pt(0)- η^2 -phosphaalkyne Complexes

- 4: R = *i*Pr, n = 2; 5: R = Cy, n = 2; 6: R = Cy, n = 1
 7: R = *i*Pr, n = 2, Ar = Mes*; 8: R = *i*Pr, n = 2, Ar = Mes;
 9: R = *i*Pr, n = 2, Ar = Mes*; 10: R = *i*Pr, n = 2, Ar = Mes;
 11: R = Cy, n = 2, Ar = Mes; 12: R = Cy, n = 2, Ar = Tripp;
 13: R = Cy, n = 1, Ar = Tripp

yellow/orange/red solids in moderate to good yields and were characterized by means of multinuclear NMR spectroscopy.

Scheme 2. Photochemical C–C Bond Activation and Thermally Induced Reverse Reaction



- 14: R = *i*Pr, n = 2, Ar = Mes; 15: R = Cy, n = 2, Ar = Mes;
 16: R = Cy, n = 2, Ar = Tripp; 17: R = Cy, n = 1, Ar = Tripp

Despite the presence of the sterically demanding Mes* group, the NMR spectroscopic data of **7** and **9** clearly show that phosphaalkyne **1** is η^2 -coordinated to the metal center. This is particularly interesting as neither Ni(0)- nor Pt(0)-complexes of this ligand have been reported before. Additionally, we could crystallographically characterize coordination compounds **8** (Ni(0), Mes-C≡P) and **12** (Pt(0), Tripp-C≡P). The results of the X-ray crystal structure analyses, along with selected bond lengths and angles, are depicted in Figures 3 and 4.

Compound **8** represents the first structurally characterized Ni(0)- η^2 -phosphaalkyne complex. In both coordination compounds **8** and **12**, the metal center adopts a square planar

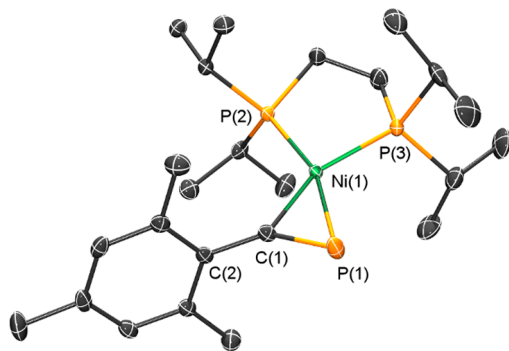


Figure 3. Molecular structure of **8** in the crystal. Displacement ellipsoids are shown at the 50% probability level. Hydrogen atoms are omitted for clarity. Selected bond lengths (Å) and angles (deg): C(1)–P(1), 1.6448(17); C(1)–C(2), 1.461(2); Ni(1)–P(1), 2.1768(5); Ni(1)–C(1), 1.8897(16); Ni(1)–P(2), 2.1573(5); Ni(1)–P(3), 2.1563(5). P(2)–Ni(1)–P(3), 91.328(18); P(1)–Ni(1)–C(1), 47.07(5); P(1)–C(1)–C(2), 142.81(13).

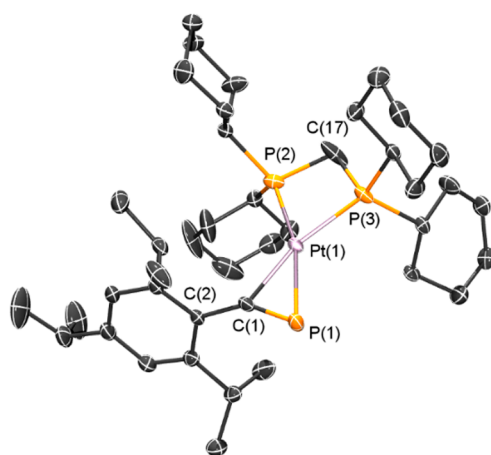


Figure 4. Molecular structure of **12** in the crystal. Displacement ellipsoids are shown at the 50% probability level. Hydrogen atoms are omitted for clarity. Disordered cyclohexyl groups shown in their preferred conformation. Selected bond lengths (Å) and angles (deg): C(1)–P(1), 1.652(2); C(1)–C(2), 1.463(3); Pt(1)–P(1), 2.3271(6); Pt(1)–C(1), 2.042(2); Pt(1)–P(2), 2.2934(6); Pt(1)–P(3), 2.2899(6). P(2)–Pt(1)–P(3), 73.52(2); P(1)–Pt(1)–C(1), 43.81(6); P(1)–C(1)–C(2), 147.55(17).

coordination geometry. The P(1)–C(1)–C(2) angle of 142.81(13)° in **8** and the P(1)–C(1)–C(2) angle of 147.55(17)° in **12** are indicative of a significant amount of π -back-donation to the π^* orbitals of the C≡P moiety. This causes enough d^8 Ni(II) and Pt(II) metallaphosphacyclopropene character to account for the preference for a square planar structure. This is also evident from the lengthening of the P(1)–C(1) bond upon coordination (1.6448(17) Å in **8** vs 1.545(3) Å in **3**).

Having synthesized a series of η^2 -phosphaalkyne complexes of Ni(0) and Pt(0), we turned our attention to the thermal C(*sp*)–C(*sp*²) bond activation. As already anticipated, both coordination compounds **7** and **9**, containing the sterically demanding Mes*-C≡P ligand **1**, do not show any oxidative addition processes at the metal center, even at prolonged heating to $T = 110$ °C. Moreover, we could also not detect any thermal C–C cleavage for complexes **8** and **10**, which are based on the sterically least demanding Mes-C≡P (**3**) in the series of investigated phosphaalkynes.

We thus focused our investigations on potential photochemical C(*sp*)–C(*sp*²) bond cleavage reactions. Again, neither the Ni(0) complexes **7** (Mes*-C≡P) and **8** (Mes-C≡P) nor the Pt(0) complex **9** (Mes*-C≡P) undergo any bond activation processes upon photolysis in toluene. In fact, compound **9** slowly decomposes after several hours of irradiation with UV light, whereas **7** and **8** seem to be stable under these conditions. Much to our delight, we could detect a considerable change in the ³¹P{¹H} NMR spectrum of the Pt(0)-complex **10** (Mes-C≡P) in THF, when it is exposed to UV light. Figure 5a shows the ³¹P{¹H} NMR spectrum of **10** in THF-*d*⁸. The spectrum clearly shows the typical resonances of the phosphorus atoms of the coligand (dippe) at δ (ppm) = 72.0 (dd) and 80.8 (dd) with the respective ¹⁹⁵Pt satellites ($J_{\text{Pt-P}} = 3211, 3056$ Hz). The phosphorus resonance of the η^2 -bound C≡P group appears at δ (ppm) = 138.3 (dd) with ¹⁹⁵Pt satellites ($J_{\text{Pt-P}} = 230$ Hz). The ¹⁹⁵Pt NMR spectrum displays a signal at δ (ppm) = –4611.1 (ddd) and confirms the detected $J_{\text{Pt-P}}$ couplings.

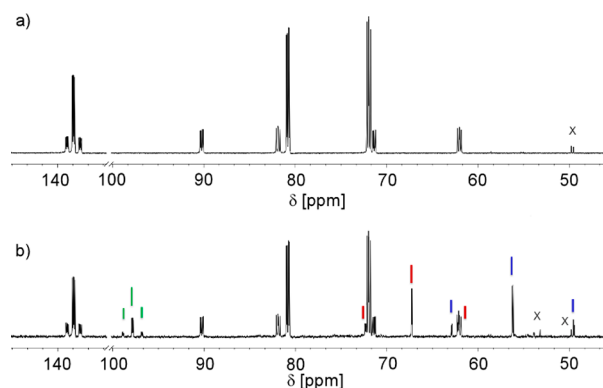


Figure 5. $^{31}\text{P}\{^1\text{H}\}$ NMR spectrum (THF- d^8) of **10** (a) and of the same sample after photolysis for 12 h (b). Signals of the new species **14** (with ^{195}Pt -satellites) in green, red, and blue. Impurities are marked with an asterisk.

Upon photolysis of **10** ($\lambda_{\text{max}} = 365$ nm, 100 W high-pressure mercury lamp) for 12 h in THF, a new set of signals was clearly visible in the $^{31}\text{P}\{^1\text{H}\}$ NMR spectrum (Figure 5b). The new compound (**14**) again shows the typical resonances for the coligand dippe at $\delta(\text{ppm}) = 56.2$ (d) and 67.3 (d) with ^{195}Pt satellites ($J_{\text{Pt-P}} = 2169$ Hz, 1653 Hz) as well as a new signal at $\delta(\text{ppm}) = 97.8$ (dd) and a $^2J_{\text{Pt-P}}$ coupling of 340 Hz, which we attribute to a σ -bound cyaphido ligand. The $J_{\text{Pt-P}}$ couplings are again verified by the corresponding ^{195}Pt NMR spectrum ($\delta(\text{ppm}) = -4476$ (ddd)). Nevertheless, we could only achieve a maximum conversion for **10** \rightarrow **14** of approximately 20%, even under prolonged photolysis. This is due to a rather fast thermal back-reaction of the σ -complex **14** to the η^2 -phosphaalkyne complex **10**, even at room temperature (Scheme 2). It should be mentioned, however, that we cannot exclude a photochemical back-reaction, in addition to the thermal reductive elimination process.

At this point, these observations already show that a photochemical $\text{C}(sp)\text{--C}(sp^2)$ bond activation reaction in η^2 -bound aryl phosphalkynes is possible, which strongly depends on the steric demand of the aryl substituent. This is in line with the observations by Weigand and González, as also the photochemical cleavage of the $\text{C}(sp)\text{--C}(sp^2)$ bond in their Pt(0)-diphenylacetylene complexes depends on the steric demand of the alkyne.⁶ In terms of reactivity, the η^2 -bound phosphalkyne is more similar to diphenylacetylene (see Chart 1) than to benzonitrile.⁴ Thermal oxidative addition does not occur for a Ni(0) phosphalkyne complex, but photochemical C–C bond cleavage, as well as thermal reductive elimination reaction, for the corresponding Pt(0)-complex does. Again, this nicely demonstrates the diagonal relationship in the periodic table of the elements between carbon and phosphorus.

Compound **10** has a lowest energy absorption around $\lambda = 400$ nm. Figure 6 displays a superimposition of the experimental UV–vis spectrum of **10** and the predicted vertical electronic excitations of this compound, derived by *ab initio* unparametrized STEOM-DLPNO–CCSD calculations (see Supporting Information (SI) for details). The calculations reveal that the absorption band at $\lambda = 398.3$ nm can be attributed mainly to an MLCT ($d_{x^2-y^2} \rightarrow \pi^*_{\text{CP}}$) and an LLCT ($\pi_{\text{Mes}} \rightarrow \pi^*_{\text{CP}}$) transition. Therefore, we anticipated that an irradiation with this specific wavelength should maximize the electronic excitation for inducing the photochemical $\text{C}(sp)\text{--}$

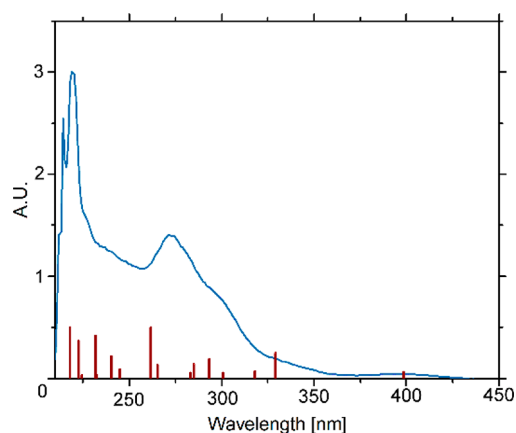


Figure 6. Experimental UV–vis spectrum (blue) and theoretical vertical excitations (red) for **10**.

$\text{C}(sp^2)$ bond activation. The corresponding density difference plot for the lowest singlet excitations is shown in Figure 7.

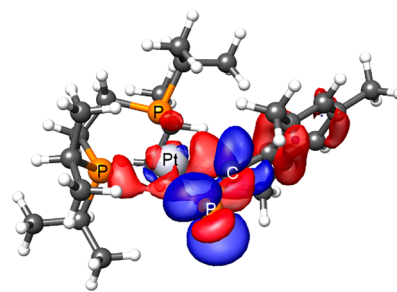


Figure 7. Density difference plot (isosurface value 0.003) for the transition at $\lambda = 398.3$ nm in **10**. The transition occurs from red to blue.

Motivated by these promising results, we further investigated the photochemical oxidative addition and the respective thermal reductive elimination reactions for the Pt(0) complexes **10–13**. There was particular focus on how the substituents at the phosphorus atoms of the coligand (R) as well as the bite angle of the coligand would influence the reactivity (Scheme 2). According to the calculations made for the electronic excitations, we changed the light source ($\lambda_{\text{max}} = 405$ nm, 4×15 W blacklight LED) to improve the outcome of the photochemical reaction. By using the chelating diphosphine dcype (**5**) as coligand, we could indeed increase the maximum conversion of **11** to the σ -complex **15** as much as 80%. By irradiating **11** in the solid state, the conversion seems to be even more efficient. In **15**, the cyaphido ligand shows a $\text{C}\equiv\text{P}$ vibrational mode at $\tilde{\nu} = 1259$ cm^{-1} in the IR spectrum. A comparison with the IR data found for the cyaphido ligand in $[\text{Ru}(\text{dppe})(\text{H})\text{C}\equiv\text{P}]$ ($\tilde{\nu} = 1228$ cm^{-1}) indicates diminished π -back-donation from the metal into the π^* -orbitals of the $\text{C}\equiv\text{P}$ fragment, as Pt(II) is “harder” than Ru(II).²⁰ However, the reverse reductive elimination reaction for **15** \rightarrow **11** is still observed at room temperature and the quantitative formation of **11** was observed within 1 h at $T = 60$ °C.

Despite the rather fast reverse reaction of **15** toward the π -complex **11**, we were able to isolate single crystals of **15**, suitable for X-ray diffraction. The result of the X-ray crystal structure analysis, along with selected bond distances and angles, is depicted in Figure 8.

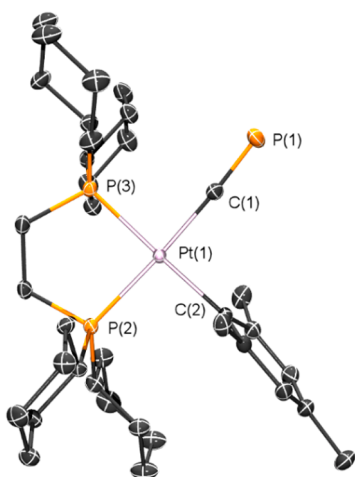


Figure 8. Molecular structure of **15** in the crystal. Displacement ellipsoids are shown at the 50% probability level. Hydrogen atoms are omitted for clarity. Selected bond lengths (Å) and angles (deg): P(1)–C(1), 1.5625(18); C(1)–Pt(1), 1.9743(18); Pt(1)–C(2), 2.0920(16); Pt(1)–P(2), 2.3153(4); Pt(1)–P(3), 2.2940(4); P(2)–Pt(1)–P(3), 85.907(15); C(1)–Pt(1)–C(2), 87.57(7); P(1)–C(1)–Pt(1), 176.62(12).

The molecular structure of **15** in the crystal unambiguously confirms the presence of a square planar Pt(II)-cyphido complex and shows, from a conceptual point of view, that a C(*sp*)–C(*sp*²) bond activation reaction in aryl-substituted phosphalkynes is possible and has been achieved for the first time. Compound **15** represents the first crystallographically characterized terminal Pt–C≡P complex. The C–P bond distance of 1.5625(18) Å is in line with the previously reported values found in Ru(II)–C≡P complexes.²⁰ Moreover, the Pt–C≡P fragment exhibits a slight distortion from linearity in the solid state (\angle Pt–C–P = 176.62(12)^o).

Subsequently, we investigated C(*sp*)–C(*sp*²) bond activation reactions for the η^2 -bound phosphalkyne Tripp–C≡P (**2**). Much to our delight, a quantitative conversion to σ -complex **16** is achieved within 1.5 h upon photolysis of **12**, while the thermally induced reductive elimination to **12** is much slower at room temperature than in the case of **14** and **15**. As coligands with smaller bite angles should generally enhance oxidative addition reactions, we finally photolyzed coordination compound **13**, consisting of the η^2 -bound Tripp–C≡P and the diphosphine dcypm, which contains a C₁ bridge.²¹ Most strikingly the σ -complex **17** is formed almost quantitatively within 18 h upon photolysis, while in this case, no back reaction toward the π -complex is observed at room temperature. Only, at *T* = 60 °C, a slow reductive elimination resulting in π -complex **13** occurs. Apparently, the combination of an aryl phosphalkyne with moderate steric demand and a small bite-angle coligand renders a much more thermodynamically stable cyphido complex. In **17**, the cyphido ligand shows a C≡P vibrational mode at $\tilde{\nu}$ = 1262 cm⁻¹ in the IR spectrum and a ³¹P{¹H} resonance at δ (ppm) = 108.9 with ¹⁹⁵Pt satellites (²*J*_{Pt–P} = 345 Hz) in the ³¹P{¹H} NMR spectrum.

We were also able to grow crystals of σ -complex **17**, which were suitable for X-ray diffraction. The result of the X-ray crystal structure analysis, along with selected bond distances and angles, is depicted in Figure 9.

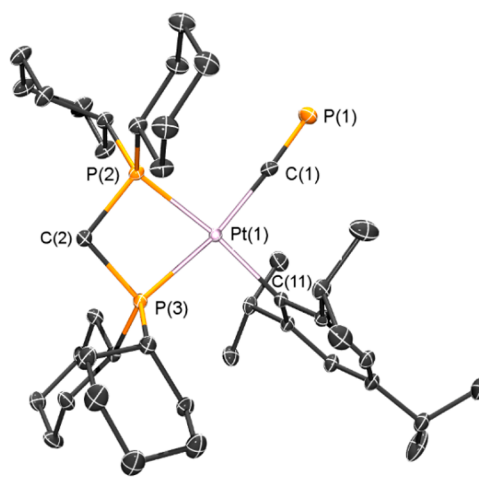


Figure 9. Molecular structure of **17** in the crystal. Displacement ellipsoids are shown at the 50% probability level. Hydrogen atoms are omitted for clarity. Only the major component is shown. Selected bond lengths (Å) and angles (deg): P(1)–C(1), 1.5553(12); C(1)–Pt(1), 1.9890(12); Pt(1)–C(11), 2.0960(11); Pt(1)–P(2), 2.3053(3); Pt(1)–P(3), 2.3126(3); P(2)–Pt(1)–P(3), 73.201(11); C(1)–Pt(1)–C(11), 89.61(5); P(1)–C(1)–Pt(1), 176.47(8).

It is worth mentioning that determining the crystal structure of compound **17** was particularly challenging and standard strategies²² were insufficient to establish the minor component of this difficult whole-molecule disorder. The concept of “archetype structures”²³ and molecule-in-cluster calculations²⁴ lead to theoretical starting coordinates. The high quality of the diffraction data for **17** made identifying and modeling fine details of the electron density distribution, namely a second component of a solid solution, possible. Starting from the largest residual electron density peak, the second site of a Pt atom was found initially. Since a nearly identical second conformation of the main component (97.5% occupancy) can be resolved, it was interpreted as a mesityl-hydrido-Pt(II) complex (2.5% occupancy, H not visible) which was confirmed to have a similar conformation by computation (SI). For modeling the diffraction data, the minor component initially required restrained refinement with structure-specific restraints.²⁵ Our final model (hydrido H omitted) is then stable without computed restraints. The discussion of the molecular geometry and chemistry within this manuscript is limited to the major component. It should be pointed out that our approach is one of the first practical applications of the archetype concept and, without it, the molecular structure of compound **17** in the crystal could not have been completed. More details about the refinement of this in addition to the other structures can be found in the SI.

To date, the herein presented synthetic procedure is the most atom-economical way to prepare cyphido complexes, as no byproducts were formed. Moreover, our observations indicate that the overall C–C≡P activation process in Pt(0) complexes is thermodynamically uphill. In order to estimate the activation barrier for the thermal reductive elimination reaction, DFT calculations (ω B97xD-D3/def2-TZVP level of theory; see SI for additional details) were performed for the model Pt(II)-complex **V** (C₁-bridge). For simplicity, this coordination compound contains the diphosphine bis-(dimethylphosphino)methane (dmpm) as the coligand in combination with Mes–C≡P (**3**). The gas phase Gibbs free

energy (ΔG^0) as well as the activation barrier (ΔG^\ddagger) for the reaction $V-\sigma \rightarrow V-\pi$ is shown in Figure 10.

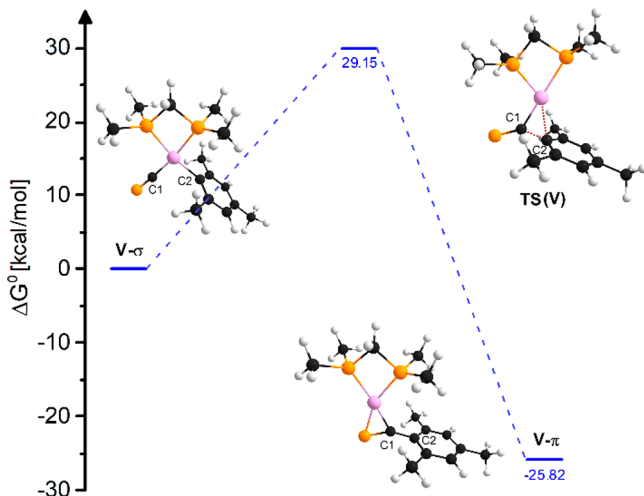


Figure 10. Energy diagram with Gibbs free energies and activation barriers of the thermal reductive elimination leading to complex $V-\pi$ (C1-bridge) calculated at the ω B97xD-D3/def2-TZVP level of theory. Relative free Gibbs energies are given in kcal/mol with respect to the σ -complex $V-\sigma$ (0 kcal/mol). Distance C1–C2 (Å): $V-\sigma$, 2.912; TS(V), 1.491; $V-\pi$, 1.456.

The energetic profile of the reaction displays an exergonic process for the reductive elimination reaction. This nicely confirms our experimental observations, that the Pt(0)- π -complexes are thermodynamically more stable than the corresponding Pt(II)-cyaphido σ -complexes ($V-\sigma \rightarrow V-\pi$: $\Delta G^0 = -25.82$ kcal/mol; $\Delta G^\ddagger = 29.15$ kcal/mol). Similar results were obtained from the calculations on model complex VI, which contains the diphosphine bis(dimethylphosphino)ethane (dmpe, C₂-bridge) as the coligand.

We also investigated the electronic structure of 17 by means of DFT calculations. The computational results closely reproduce the bond lengths and angles found in the X-ray data of 17, and Figure 11 shows a representation of the frontier orbitals of the Pt(II)-cyaphido complex.

Interestingly, and in contrast to the observations made by Crossley and co-workers on $L_nRu-C\equiv P$ complexes, the phosphorus atom of the $C\equiv P$ ligand contributes significantly to the LUMO and lies 8.50 eV above the HOMO. A rather high contribution of the $\pi_{C\equiv P}$ can be found in the HOMO-1 (-7.96 eV) and HOMO-3 (-8.34 eV). Moreover, the lone pair of the terminal phosphorus atom has a significant contribution to the HOMO-6 (-9.33 eV) and is much higher in energy when compared to $L_nRu-C\equiv P$ complexes, with a stabilization of ca. 1.64 eV with respect to the HOMO. We anticipated that these findings are important for subsequent follow-up reactions at the $C\equiv P$ ligand, as the computational results indicate that reactions with nucleophiles at the phosphorus atom and with electrophiles at both the $C\equiv P-\pi$ -system and the phosphorus lone pair might be possible. Moreover, it is obvious from Figures 8, 9, and 11 that the rather facile accessibility of the cyaphido moiety in the square planar Pt(II)-complexes should allow for the first time for cycloaddition reactions with the $C\equiv P-\pi$ -system.

Consequently, we challenged the novel σ -complex 15 for a reaction with Dipp-N₃ (Dipp = diisopropylphenyl), as classical

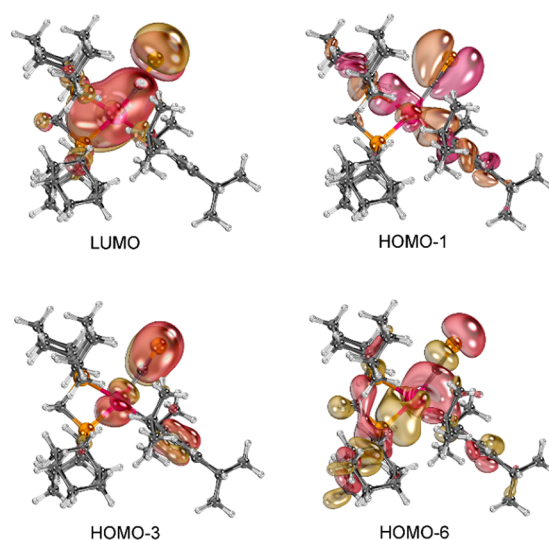


Figure 11. Frontier molecular orbitals of 17. The same perspective was chosen as in Figure 9.

phosphaalkynes undergo regioselective [3 + 2] cycloaddition reactions with organic azides under formation of triazaphospholes.²⁶ As described above, σ -complex 15 was first generated *in situ* by photolysis of 11 for 1.5 h ($\lambda = 405$ nm) in THF. Subsequently, Dipp-N₃ (1 equiv) was added and the reaction mixture was stirred overnight at room temperature.

Much to our delight, we could observe the selective and quantitative formation of a new species by means of NMR spectroscopy. This compound shows the resonances for the coligand dcpe at δ (ppm) = 50.3 (d) and 59.0 (d) with ¹⁹⁵Pt satellites (¹J_{Pt-P} = 1805 Hz, 2020 Hz) as well as a new signal at δ (ppm) = 210.9 (dd) and a ²J_{Pt-P} coupling of 510 Hz, which we attribute to the anionic triazaphospholato ligand. The J_{Pt-P} couplings are again verified by the corresponding ¹⁹⁵Pt NMR spectrum (δ (ppm) = -4509 (ddd)).

Crystals suitable for X-ray analysis could be obtained from the reaction product by slow concentration of a saturated *n*-hexane solution. The result of the crystallographic characterization is depicted in Figure 12 and shows that the Pt(II) complex 18 had been formed (see Scheme 3).

Coordination compound 18 is the first reported complex containing an anionic triazaphospholato ligand. The crystallographic data confirm that the [3 + 2] cycloaddition of an azide to the cyaphido ligand proceeded in a regioselective manner, akin to what is observed for the reaction of a phosphaalkyne with organic azides. The bond lengths and angles within the triazaphospholato heterocycle are only marginally different compared to the values found for neutral 3,5-disubstituted 3H-1,2,3,4-triazaphosphole derivatives.²⁷ According to the isolobal relationship between a CH group and a trivalent phosphorus atom, this reaction is related to the [3 + 2] cycloaddition of organic azides to metal-acetylides.²⁸ Most importantly, our results demonstrate not only that the cyaphido ligand can be generated by a photochemical C–C bond activation reaction, starting from aryl-substituted phosphaalkynes, but also that follow-up reactions at the $C\equiv P$ moiety are possible.

3. CONCLUSIONS

In conclusion, we could achieve for the first time a photochemical C(sp)–C(sp²) bond activation in η^2 -coordinated aryl phosphaalkynes, leading selectively to Pt(II)-

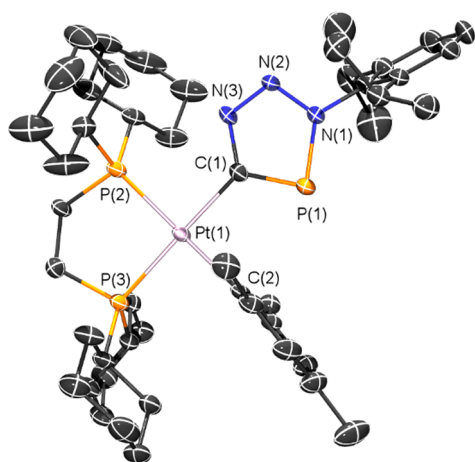
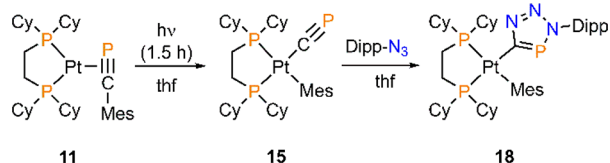


Figure 12. Molecular structure of **18** in the crystal. Displacement ellipsoids are shown at the 50% probability level. Hydrogen atoms are omitted for clarity. Only one molecule in the asymmetric unit is shown. Average selected bond lengths (Å) and angles (deg): P(1)–C(1), 1.716(6); C(1)–Pt(1), 2.044(7); Pt(1)–C(2), 2.084(66); Pt(1)–P(2), 2.2905(16); Pt(1)–P(3), 2.3023(18). P(2)–Pt(1)–P(3), 86.69(6); C(1)–Pt(1)–C(2), 86.1(3); P(1)–C(1)–Pt(1), 124.4 (4).

Scheme 3. [3 + 2] Cycloaddition Reaction of **15 with an Organic Azide and Selective Formation of the Pt(II)-Triazapospholato Complex **18****



cyphido complexes in a clean and atom-economic way. As verified experimentally and by means of theoretical calculations, the oxidative addition reaction at the Pt(0) center is thermodynamically uphill, as the σ -cyphido complexes are quantitatively converted back to the corresponding Pt(0)- π -complexes upon heating. In accordance with the diagonal relationship between phosphorus and carbon in the periodic table of the elements, the hitherto unknown C(sp)–C(sp^2) in aryl phosphalkynes is similar to the photochemical oxidative addition of aryl alkynes in Pt(0) complexes. Furthermore, we could demonstrate, for the first time, that Pt(II)–C \equiv P complexes are rather reactive. In the presence of an organic azide, we could prove that the corresponding [3 + 2] cycloaddition product can be obtained selectively. Our first results provide the possibility to investigate the follow-up chemistry of Pt-cyphido complexes in more detail and to transfer our observations also to arsaalkynes and the cyarsido ligand (C \equiv As $^-$). Moreover, experimental and computational studies are currently performed in our laboratories in order to unravel the mechanism of the photochemical C(sp)–C(sp^2) bond activation reaction in aryl phosphalkynes.

4. EXPERIMENTAL SECTION

The experimental details for the formation of complexes **14**–**17** are given below. For general considerations and synthesis of the precursors, please see the SI.

General Setup for the Irradiation of π -Pt Complexes **9–**13** To Form σ -Pt Complexes (**14**–**17**).** The π -Pt complex (**9**–**13**,

24.4–122 μ mol) was dissolved in THF (1–5 mL) and transferred into either a J. Young NMR tube or a thin Schlenk tube equipped with a magnetic stirring bar and placed in the middle of a setup of four 15 W backlight LED array (λ_{\max} = 405 nm) with a distance to the tube of about 5 cm. The irradiation was performed at room temperature (lower temperature favors the formation of σ -Pt complex). Depending on the π -Pt complex (**9**–**13**) used, the reaction time varies from 1.5 to 18 h.

Additional Remarks. In the following, the typical conversion ratio from the π -Pt to the σ -Pt complex at room temperature is given as a percentage. According to NMR studies there are no side products, and all unreacted π -Pt complexes stay unchanged in solution. The oxidative addition reaction (irradiation) and reductive elimination (thermal back reaction) can be repeated several times without showing any side products in the NMR spectrum for a pure sample. The exception to this is for the conversion between **13** and **17** (both directions). This system releases dcypm (**6**) and also TrippCP (**2**), which undergoes further unspecific side reactions upon irradiation.

[(dippe)Pt(Mes)(CP)] (14**).** Irradiation of **10** for 1.5 h gives 70% conversion. ^1H NMR (700 MHz, tetrahydrofuran- d_8): δ = 6.55 (s, 2H, *meta*-H-Mes), 2.43 (s, 6H, *ortho*-CH $_3$ -Mes), 2.11 (s, 3H, *para*-CH $_3$ -Mes), 2.68 (dq, $^2J_{\text{H,P}}$ = 16.4 Hz, $^3J_{\text{H,H}}$ = 7.11 Hz, 2H, P–CH), 2.12 (dq, $^2J_{\text{H,P}}$ = 15.8 Hz, $^3J_{\text{H,H}}$ = 7.03 Hz, 2H, P–CH), 1.75 (m, 4H, P–CH $_2$), 1.45 (dd, $^3J_{\text{H,P}}$ = 16.1 Hz, $^2J_{\text{H,H}}$ = 7.17 Hz, 6H, CH $_3$ of ^iPr), 1.22 (dd, $^3J_{\text{H,P}}$ = 13.5 Hz, $^2J_{\text{H,H}}$ = 7.06 Hz, 6H, CH $_3$ of ^iPr), 1.07 (dd, $^3J_{\text{H,P}}$ = 13.8 Hz, $^2J_{\text{H,H}}$ = 6.97 Hz, 6H, CH $_3$ of ^iPr), 0.89 (dd, $^3J_{\text{H,P}}$ = 15.1 Hz, $^2J_{\text{H,H}}$ = 7.20 Hz, 6H, CH $_3$ of ^iPr) ppm. $^{13}\text{C}\{^1\text{H}\}$ NMR (176 MHz, tetrahydrofuran- d_8): δ = 232.7 (app. dt, J = 114.3, 10.5 Hz, CP), 153.9 (dd, J = 102.4, 8.64 Hz, *ipso*-C-Mes), 143.5 (Mes), 131.3 (Mes), 128.0 (Mes), 27.4 (d, J = 3.6 Hz), 25.9, 22.7, 19.4, 19.1 (d, J = 2.6 Hz), 18.9, 18.0 ppm. $^{31}\text{P}\{^1\text{H}\}$ NMR (162 MHz, tetrahydrofuran- d_8): δ = 99.0 (dd, $^3J_{\text{P,P}}$ = 18.2, 10.7 Hz, $^1J_{\text{P,Pt}}$ = 340 Hz, CP), 68.9 (d, $^2,^3J_{\text{P,P}}$ = 10.7 Hz, $^1J_{\text{P,Pt}}$ = 1653 Hz, dippe), 57.9 (d, $^2,^3J_{\text{P,P}}$ = 18.0 Hz, $^1J_{\text{P,Pt}}$ = 2169 Hz, dippe) ppm. $^{195}\text{Pt}\{^1\text{H}\}$ NMR (86 MHz, tetrahydrofuran- d_8): δ = –4476 (ddd, $^1J_{\text{P,Pt}}$ = 2169, 1653, 340 Hz) ppm. IR: $\tilde{\nu}$ = 1242 (C \equiv P) cm^{-1} .

[(dcype)Pt(Mes)(CP)] (15**).** Irradiation of **11** for 1.5 h gives 80% conversion. ^1H NMR (400 MHz, tetrahydrofuran- d_8): δ = 6.78 (s, 2H, *meta*-H-Mes), 2.45 (s, 6H, *ortho*-CH $_3$ -Mes), 2.13 (s, 3H, *para*-CH $_3$ -Mes), 2.33–0.69 (m, 48H, P–CH, P–CH $_2$, Cy) ppm. $^{31}\text{P}\{^1\text{H}\}$ NMR (162 MHz, tetrahydrofuran- d_8): δ = 96.6 (dd, $^3J_{\text{P,P}}$ = 17.7, 10.4 Hz, $^1J_{\text{P,Pt}}$ = 338 Hz, CP), 60.2 (d, $^2,^3J_{\text{P,P}}$ = 10.3 Hz, $^1J_{\text{P,Pt}}$ = 1654 Hz, dcype), 49.2 (d, $^2,^3J_{\text{P,P}}$ = 17.8 Hz, $^1J_{\text{P,Pt}}$ = 2164 Hz, dcype) ppm. $^{195}\text{Pt}\{^1\text{H}\}$ NMR (86 MHz, tetrahydrofuran- d_8): δ = –4463 (ddd, $^1J_{\text{P,Pt}}$ = 2164, 1654, 338 Hz) ppm. IR: $\tilde{\nu}$ = 1259 (C \equiv P) cm^{-1} .

[(dcype)Pt(Tripp)(CP)] (16**).** Irradiation of **12** for 3 h gives quantitative conversion. ^1H NMR (600 MHz, tetrahydrofuran- d_8): δ = 6.75 (s, 2H, *meta*-H-Tripp), 3.71 (hept., $^3J_{\text{H,H}}$ = 6.78 Hz, 2H, *ortho*-CH-Tripp), 2.74 (hept., $^3J_{\text{H,H}}$ = 6.90 Hz, 1H, *para*-CH-Tripp), 1.20–1.38 (dd J = 18.33, 6.77 Hz, d, $^3J_{\text{H,H}}$ = 6.90 Hz, 18H, *ortho*- and *para*-CH $_3$ -Tripp), 2.33–0.67 (m, 48H, P–CH, P–CH $_2$, Cy) ppm. $^{13}\text{C}\{^1\text{H}\}$ NMR (151 MHz, tetrahydrofuran- d_8): δ = 225.5 (d, J = 117.8 Hz, CP), 155.0, 152.3 (dd, J = 102.0, 8.7 Hz, Tripp), 144.1 (Tripp), 120.5 (Tripp), 37.2, 34.8 (d, J = 25.6 Hz), 34.3 (d, J = 26.9 Hz), 30.3, 29.9 (d, J = 5.9 Hz), 29.1, 27.8 (d, J = 10.0 Hz), 27.5 (d, J = 16.6 Hz), 26.8, 24.2, 23.3 (dt, J = 27.4, 13.7 Hz), 22.6 (dd, 25.0, 10.4 Hz) ppm. $^{31}\text{P}\{^1\text{H}\}$ NMR (162 MHz, tetrahydrofuran- d_8): δ = 108.9 (dd, $^3J_{\text{P,P}}$ = 18.2, 10.7 Hz, $^1J_{\text{P,Pt}}$ = 331 Hz, CP), 60.9 (d, $^2,^3J_{\text{P,P}}$ = 10.6 Hz, $^1J_{\text{P,Pt}}$ = 1647 Hz, dcype), 48.6 (d, $^2,^3J_{\text{P,P}}$ = 17.5 Hz, $^1J_{\text{P,Pt}}$ = 2145 Hz, dcype) ppm. $^{195}\text{Pt}\{^1\text{H}\}$ NMR (86 MHz, tetrahydrofuran- d_8): δ = –4393 (ddd, $^1J_{\text{P,Pt}}$ = 2145, 1647, 331 Hz) ppm. IR: $\tilde{\nu}$ = 1260 (C \equiv P) cm^{-1} .

[(dcypm)Pt(Tripp)(CP)] (17**).** Irradiation of **13** for 18 h gives 95% conversion. ^1H NMR (700 MHz, tetrahydrofuran- d_8): δ = 6.67 (s, 2H, *meta*-H-Tripp), 3.23 (hept., $^3J_{\text{H,H}}$ = 6.79 Hz, 2H, *ortho*-CH-Tripp), 3.23 (t, $^2J_{\text{H,P}}$ = 8.7 Hz, 2H, P–CH $_2$ –P), 2.71 (hept., $^3J_{\text{H,H}}$ = 6.90 Hz, 1H, *para*-CH-Tripp), 1.34 (dd, J = 22.43, 6.84 Hz, 6H, *para*-CH $_3$ -Tripp), 1.19 (dd, J = 15.58, 6.83 Hz, 12H, *ortho*-CH $_3$ -Tripp), 2.08–0.87 (m, 44H, P–CH, Cy) ppm. $^{13}\text{C}\{^1\text{H}\}$ NMR (176 MHz,

tetrahydrofuran- d_8): δ = 222.7 (app. d, J = 122.1 Hz, CP), 151.3 (Tripp), 151.8 (dd, J = 110.4, 5.1 Hz, Tripp), 143.6 (Tripp), 119.9 (Tripp), 37.6 (d, J = 3.4 Hz), 36.2 (dd, J = 15.1, 4.4 Hz), 35.2, 34.9 (dd, J = 15.8, 5.3 Hz), 29.9 (d, J = 6.1 Hz), 29.3, 28.2 (d, J = 3.5 Hz), 28.1 (d, J = 2.2 Hz), 28.0, 27.9, 27.7 (d, J = 10.5 Hz), 27.2 (J = 4.4 Hz), 26.8, 24.4 ppm. $^{31}\text{P}\{^1\text{H}\}$ NMR (162 MHz, tetrahydrofuran- d_8): δ = 110.5 (dd, $^3J_{\text{P,P}} = 18.8$, 11.2 Hz, $^1J_{\text{P,Pt}} = 345$ Hz, CP), -29.1 (dd, $^{2,3}J_{\text{P,P}} = 30.2$, 10.2 Hz, $^1J_{\text{P,Pt}} = 1343$ Hz, dcpm), -38.2 (dd, $^{2,3}J_{\text{P,P}} = 30.2$, 18.5 Hz, $^1J_{\text{P,Pt}} = 1824$ Hz, dcpm) ppm. $^{195}\text{Pt}\{^1\text{H}\}$ NMR (86 MHz, tetrahydrofuran- d_8): δ = -3792 (ddd, $^1J_{\text{Pt,P}} = 1824$, 1343 , 345 Hz) ppm. IR: $\tilde{\nu}$ = 1262 (C \equiv P) cm^{-1} .

■ ASSOCIATED CONTENT

Supporting Information

The Supporting Information is available free of charge at <https://pubs.acs.org/doi/10.1021/jacs.1c07370>.

Details on experimental procedures, the X-ray crystal structure analyses, and DFT calculations are given. (PDF)

Accession Codes

CCDC 2096680 and 2096826–2096830 contain the supplementary crystallographic data for this paper. These data can be obtained free of charge via www.ccdc.cam.ac.uk/data_request/cif, or by emailing data_request@ccdc.cam.ac.uk, or by contacting The Cambridge Crystallographic Data Centre, 12 Union Road, Cambridge CB2 1EZ, UK; fax: +44 1223 336033.

■ AUTHOR INFORMATION

Corresponding Authors

William D. Jones – Department of Chemistry, University of Rochester, Rochester, New York 14627, United States; orcid.org/0000-0003-1932-0963; Email: wjones@ur.rochester.edu

Christian Müller – Freie Universität Berlin, Institut für Chemie und Biochemie, 14195 Berlin, Germany; orcid.org/0000-0003-4700-0502; Email: c.mueller@fu-berlin.de

Authors

Tim Görlich – Freie Universität Berlin, Institut für Chemie und Biochemie, 14195 Berlin, Germany

Daniel S. Frost – Freie Universität Berlin, Institut für Chemie und Biochemie, 14195 Berlin, Germany

Nico Boback – Freie Universität Berlin, Institut für Chemie und Biochemie, 14195 Berlin, Germany

Nathan T. Coles – Freie Universität Berlin, Institut für Chemie und Biochemie, 14195 Berlin, Germany; orcid.org/0000-0001-6190-9080

Birger Dittich – Mathematisch-Naturwissenschaftliche Fakultät, Universität Zürich, Zürich CH-8057, Switzerland

Peter Müller – Massachusetts Institute of Technology, Department of Chemistry, Cambridge, Massachusetts 02139-4307, United States; orcid.org/0000-0001-6530-3852

Complete contact information is available at: <https://pubs.acs.org/doi/10.1021/jacs.1c07370>

Notes

The authors declare no competing financial interest.

■ ACKNOWLEDGMENTS

Funding by Freie Universität Berlin and the Deutsche Forschungsgemeinschaft DFG is gratefully acknowledged. The authors thank the Scientific Computing Service of Freie

Universität Berlin ([10.17169/refubium-26754](https://doi.org/10.17169/refubium-26754)) for the use of high-performance computing resources. W.D.J. acknowledges support from the Alexander von Humboldt Foundation and the U.S. Department of Energy, Basic Energy Sciences (BES) Chemical Sciences, Geosciences, & Biosciences (CSGB) Division, for financial support (DE-SC0020230). The authors thank Prof. Klaus Koch (Stellenbosch University, South Africa; death January 2, 2020) for his help and support in recording the ^{195}Pt NMR spectra.

■ REFERENCES

- (1) (a) Dunbar, K. R.; Heintz, R. A. Chemistry of Transition Metal Cyanide Compounds: Modern Perspectives. *Prog. Inorg. Chem.* **2007**, *45*, 283–391. (b) Hanusa, T. P. Cyanide Complexes of the Transition Metals, in *Encyclopedia of Inorganic Chemistry-II*; John Wiley & Sons, LTD, 2006; pp 1–11.
- (2) Tolman, C. R.; McKinney, R. J.; Seidel, W. C.; Druliner, J. D.; Stevens, W. R. Homogeneous Nickel-Catalyzed Olefin Hydrocyanation. *Adv. Catal.* **1985**, *33*, 1–46.
- (3) (a) Gerlach, D. H.; Kane, A. R.; Parshall, G. W.; Jesson, J. P.; Muetterties, E. L. Reactivity of Trialkylphosphine Complexes of Platinum(0). *J. Am. Chem. Soc.* **1971**, *93*, 3543–3544. (b) Parshall, G. W. σ -Aryl Compounds of Nickel, Palladium, and Platinum. Synthesis and Bonding Studies. *J. Am. Chem. Soc.* **1974**, *96*, 2360–2366. (c) Morvillo, A.; Turco, A. Reactions of organic halides and cyanides with bis(tricyclohexylphosphine)nickel(0). *J. Organomet. Chem.* **1981**, *208*, 103–113. (d) Favero, G.; Morvillo, A.; Turco, A. Oxidative addition of alkanenitriles to nickel(0) complexes via π -intermediates. *J. Organomet. Chem.* **1983**, *241*, 251–257. (e) Schaub, T.; Döring, C.; Radius, U. Efficient nickel mediated carbon–carbon bond cleavage of organonitriles. *Dalton Trans.* **2007**, 1993–2002.
- (4) Garcia, J. J.; Jones, W. D. Reversible Cleavage of Carbon-Carbon Bonds in Benzonitrile Using Nickel(0). *Organometallics* **2000**, *19*, 5544–5545.
- (5) Müller, C.; Iverson, C. N.; Lachicotte, R. J.; Jones, W. D. Carbon-Carbon Bond Activation in Pt(0)-Diphenylacetylene Complexes Bearing Chelating P,N- and P,P-Ligands. *J. Am. Chem. Soc.* **2001**, *123*, 9718–9719.
- (6) (a) Petzold, H.; Weisheit, T.; Görls, H.; Breitzke, H.; Buntkowsky, G.; Escudero, D.; González, L.; Weigand, W. Selective carbon–carbon bond cleavage of 2,2'-dibromotolane via photolysis of its appropriate (diphosphine)Pt⁰ complex in the solid state. *Dalton Trans.* **2008**, 1979–1981. (b) Escudero, D.; Assmann, M.; Pospiech, A.; Weigand, W.; González, L. Substituent effects on the light-induced C–C and C–Br bond activation in (bisphosphine)(η^2 -tolane)Pt⁰ complexes. A TD-DFT study. *Phys. Chem. Chem. Phys.* **2009**, *11*, 4593–4600. (c) Escudero, D.; Weisheit, T.; Weigand, W.; González, L. Photochemical behavior of (bisphosphine)(η^2 -tolane)Pt⁰ complexes. Part B: An insight from DFT calculations. *Dalton Trans.* **2010**, 39, 9505–9513.
- (7) (a) Gunay, A.; Jones, W. D. Cleavage of Carbon-Carbon Bonds of Diphenylacetylene and Its Derivatives via Photolysis of Pt Complexes: Tuning the C–C Bond Formation Energy toward Selective C–C Bond Activation. *J. Am. Chem. Soc.* **2007**, *129*, 8729–8735. (b) Gunay, A.; Brennessel, W. W.; Jones, W. D. Investigation of C–C Bond Activation of sp–sp² C–C Bonds of Acetylene Derivatives via Photolysis of Pt Complexes. *Organometallics* **2015**, *34*, 2233–2239.
- (8) Dillon, K. B.; Mathey, F.; Nixon, J. F. *Phosphorus: The Carbon Copy. From Organophosphorus To Phospha-Organic Chemistry*; John Wiley & Sons: Chichester, U.K., 1998.
- (9) Jun, H.; Young, V. G.; Angelici, R. J. Phosphorus Analogue (C \equiv P[–]) of a Bridging Cyanide (C \equiv N[–]) Ligand: Synthesis and Structure of (Cl)(PEt₃)₂Pt(μ -C = P)Pt(PEt₃)₂. *J. Am. Chem. Soc.* **1992**, *114*, 10064–10065.
- (10) (a) Cordaro, J. G.; Stein, D.; Rüegger, H.; Grützmaier, H. Making the True “CP” Ligand. *Angew. Chem., Int. Ed.* **2006**, *45*, 6159–6162. (b) Ehlers, A.; Cordaro, J.-G.; Stein, D.; Grützmaier, H.

Mechanisms of Cyaphide ($C\equiv P^-$) Formation. *Angew. Chem., Int. Ed.* **2007**, *46*, 7878–7881.

(11) (a) Trathen, N.; Leech, M. C.; Crossley, I. R.; Greenacre, V. K.; Roe, S. M. Synthesis and electronic structure of the first cyaphide-alkynyl complexes. *Dalton Trans.* **2014**, *43*, 9004–9007. (b) Leech, M. C.; Crossley, I. R. Through-conjugation of two phosphalkyne ($C\equiv P$) moieties mediated by a bimetallic scaffold. *Dalton Trans.* **2018**, *47*, 4428–4432. (c) Furfari, S. K.; Leech, M. C.; Trathen, N.; Levis, M. C.; Crossley, I. R. Cyaphide-alkynyl complexes: metal-ligand conjugation and the influence of remote substituents. *Dalton Trans.* **2019**, *48*, 8131–8143.

(12) Mansell, S. M.; Green, M.; Russell, C. A. Coordination chemistry of trimethylsilylphosphalkyne: a phosphalkyne bearing a reactive substituent. *Dalton Trans.* **2012**, *41*, 14360–14368.

(13) Finze, M.; Bernhardt, E.; Willner, H.; Lehmann, C. W. $[(CF_3)_3BCP]^-$ and $[(CF_3)_3BCAs]^-$: Thermally Stable Phosphaethynyl and Arsaethynyl Complexes. *Angew. Chem., Int. Ed.* **2004**, *43*, 4160–4163.

(14) Becker, G.; Gresser, G.; Uhl, W. Acyl- und Alkylidenphosphane, XV [1] 2,2-Dimethylpropylidindiphosphan, eine stabile Verbindung mit einem Phosphoratom der Koordinationszahl 1. *Z. Naturforsch., B: J. Chem. Sci.* **1981**, *36*, 16–19.

(15) Hoerger, C. J.; Heinemann, F. W.; Louyriac, E.; Rigo, M.; Maron, L.; Grützmacher, H.; Driess, M.; Meyer, K. Cyarside (CAs^-) and 1,3-Diarsaallendiide ($AsCAs^2-$) Ligands Coordinated to Uranium and Generated via Activation of the Arsaethynolate Ligand ($OCAs^-$). *Angew. Chem., Int. Ed.* **2019**, *58*, 1679–1683.

(16) (a) Wilson, D. W. N.; Urwin, S. J.; Yang, E. S.; Goicoechea, J. M. A Cyaphide Transfer Reagent. *J. Am. Chem. Soc.* **2021**, *143*, 10367–10373. (b) Rösch, B.; Harder, S. New horizons in low oxidation state group 2 metal chemistry. *Chem. Commun.* **2021**, *57*, 9354–9365.

(17) Burckett-St. Laurent, J. C. T. R.; Hitchcock, P. B.; Kroto, H. W.; Nixon, J. F. Novel transition metal phosphalkyne complexes. X-Ray crystal and molecular structure of a side-bonded $Bu^tC\equiv P$ complex of zerovalent platinum, $Pt(PPh_3)_2(Bu^tCP)$. *J. Chem. Soc., Chem. Commun.* **1981**, 1141–1143.

(18) Märkl, G.; Sejpka, H. 2-(2,4,6-Tri-*tert*-Butylphenyl)-1-phosphaethin, 1,4-bis-(trimethylsilyloxy)-1,4-bis-(2,4,6-tri-*tert*-butylphenyl)-2,3-diphosphabutadien. *Tetrahedron Lett.* **1986**, *27*, 171–174.

(19) (a) Mack, A.; Pierron, E.; Allspach, T.; Bergsträßer, U.; Regitz, M. Organophosphorus Compounds; 129.¹ Mesitylphosphaacetylene: Synthesis and Reactivity Studies of a New Phosphalkyne. *Synthesis* **1998**, *1998*, 1305–1313. (b) Himmel, D.; Seitz, M.; Scheer, M. Beiträge zum Reaktionsverhalten von Phosphalkinen gegenüber Übergangsmetallkomplexen-Synthese und Kristallstrukturanalyse von $[(Ph_3P)_2Pt(\eta^2-PCMes)]$, $[M(CO)_3(\eta^4-P_2C_2Mes_2)]$ ($M = Fe, Ru$), $[Cp^*Mo(CO)Cl(\eta^4-P_2C_2^tBu_2)]$ und $[K(tol)_2]_2[Mn(CO)_4\{Mn(CO)_3(\eta^4-P_2C_2^tBu_2)\}_2]$. *Z. Anorg. Allg. Chem.* **2004**, *630*, 1220–1228. (c) Gläsel, T.; Jiao, H.; Hapke, M. Synthesis of Phosphinines from Co(I)-Catalyzed [2 + 2+2] Cycloaddition Reactions. *ACS Catal.* **2021**, *11*, 13434–13444.

(20) For comparison reasons, the structurally related cyanido-complex $[(dippe)Pt(Ph)C\equiv N]$ shows a $C\equiv N$ vibrational mode at $\tilde{\nu} = 2278\text{ cm}^{-1}$.

(21) (a) Hofmann, P.; Unfried, G. Room-Temperature C-F Bond Activation of Hexafluorobenzene by a Tailor-Made Pt(0) Intermediate, $[(dtpbm)Pt(0)]$. *Chem. Ber.* **1992**, *125*, 659–661. (b) Massera, C.; Frenking, G. Energy Partitioning Analysis of the Bonding in $L_2TM-C_2H_2$ and $L_2TM-C_2H_4$ ($TM = Ni, Pd, Pt$; $L_2 = (PH_3)_2, (PMe_3)_2, H_2PCH_2PH_2, H_2P(CH_2)_2PH_2$). *Organometallics* **2003**, *22*, 2758–2765.

(22) Müller, P. Practical suggestions for better crystal structures. *Crystallogr. Rev.* **2009**, *15*, 57–83.

(23) Dittrich, B. On modelling disordered crystal structures through restraints from molecule-in-cluster computations, and distinguishing static and dynamic disorder. *IUCrJ* **2021**, *8*, 305–318.

(24) Dittrich, B.; Chan, S.; Wiggan, S.; Stevens, J. S.; Pidcock, E. Fast energy minimization of the CCDC drug-subset structures by

molecule-in-cluster computations allows independent structure validation and model completion. *CrystEngComm* **2020**, *22*, 7420–7431.

(25) Sheldrick, G. M. Crystal structure refinement with SHELXL. *Acta Crystallogr., Sect. C: Struct. Chem.* **2015**, *C71*, 3–8.

(26) (a) Ko, Y. Y. C. Y. L.; Carrié, R.; Muench, A.; Becker, G. One Co-ordinate Phosphorus Compounds: 1,3-Dipolar Cycloadditions with 2,2-Dimethylpropylidynylphosphine. *J. Chem. Soc., Chem. Commun.* **1984**, 1634–1635. (b) Rösch, W.; Regitz, M. [3 + 2]-Cycloaddition Reactions of a Stable Phosphalkyne-Transition from Singly to Doubly Coordinated Phosphorus. *Angew. Chem., Int. Ed. Engl.* **1984**, *23*, 900–901.

(27) Sklorz, J. A. W.; Hoof, S.; Rades, N.; De Rycke, N.; Könczöl, L.; Szieberth, D.; Weber, M.; Wiecko, J.; Nyulászi, L.; Hissler, M.; Müller, C. Pyridyl-Functionalized 3H-1,2,3,4-Triazaphospholes: Synthesis, Coordination Chemistry and Photophysical Properties of Low-Coordinate Phosphorus Compounds. *Chem. - Eur. J.* **2015**, *21*, 11096–11109.

(28) See for example: (a) Del Castillo, T. J.; Sarkar, S.; Abboud, K. A.; Veige, A. S. 1,3-Dipolar cycloaddition between a metal-azide (Ph_3PAuN_3) and a metal-acetylide ($Ph_3PAuC\equiv CPh$): an inorganic version of a click reaction. *Dalton Trans.* **2011**, *40*, 8140–8144.

(b) Lo, Y.-H.; Wang, T.-H.; Lee, C.-Y.; Feng, Y.-H. Preparation, Characterization, and Reactivity of Azido Complex Containing a $Tp^t(BuNC)(PPh_3)Ru$ Fragment and Ruthenium-Catalyzed Cycloaddition of Organic Azides with Alkynes in Organic and Aqueous Media. *Organometallics* **2012**, *31*, 6887–6899. (c) Casarrubios, L.; de la Torre, M. C.; Sierra, M. A. The “Click” Reaction Involving Metal Azides, Metal Alkynes, or Both: An Exploration into Multimetal Structures. *Chem. - Eur. J.* **2013**, *19*, 3534–3541. (d) Beto, C. C.; Holt, E. D.; Yang, Y.; Ghiviriga, I.; Schanze, K. S.; Veige, A. S. A new synthetic route to in-chain metallopolymers via copper(I) catalyzed azide-platinum-acetylide iClick. *Chem. Commun.* **2017**, *53*, 9934–9937.